Hydrogen storage properties of Li-decorated B_2S monolayers: a DFT study

Zhiyang Liu[a,b,c], Shi Liu[a], Süleyman Er[c,d*]

[a] *Institute of Metal Research, Chinese Academy of Sciences, 72 Wenhua Road, Shenyang, 110016, China*

[b] *School of Materials Science and Engineering, University of Science and Technology of China, 72 Wenhua Road, Shenyang, 110016, China*

[c] *DIFFER – Dutch Institute for Fundamental Energy Research, De Zaale 20, 5612 AJ Eindhoven, the Netherlands*

[d] *Center for Computational Energy Research, DIFFER – Dutch Institute for Fundamental Energy Research, De Zaale 20, 5612 AJ Eindhoven, the Netherlands*

* Corresponding author: Telephone: +31(0) 40 333 4936; E-mail: s.er@differ.nl

Abstract

Hydrogen storage properties of Li functionalized B_2S honeycomb monolayers are studied using density functional theory calculations. The binding of H_2 molecules to the clean B_2S sheet proceeds through physisorption. Dispersed Li atoms on the monolayer surface increase both the hydrogen binding energies and the hydrogen storage capacities significantly. Additionally, *ab initio* molecular dynamics calculations show that there is no kinetic barrier during H_2 desorption from lithiated B_2S. Among the studied $B_8S_4Li_x$ (x = 1, 2, 4, and 12) compounds, the $B_8S_4Li_4$ is found to be the most promising candidate for hydrogen storage purposes; with a 9.1 wt% H_2 content and 0.14 eV/H_2 average hydrogen binding energy. Furthermore, a detailed analysis of the electronic properties of the $B_8S_4Li_4$ compound before and after H_2 molecule adsorption confirms that the interactions between Li and H_2 molecules are of electrostatic nature.

Keywords

DFT; 2D materials; B_2S; Li; Molecular hydrogen storage

1. Introduction

Hydrogen is an energy carrier that has attracted interest in recent years. Using the electricity generated by renewable sources, hydrogen can be produced from water. It can also be fed to a fuel cell to generate electricity when needed, such as in fuel cell electric vehicles.[1] A key issue for the efficient utilization of hydrogen is storing it at practical conditions with high gravimetric and volumetric densities.[2, 3]

The chemical composition of storage materials has a direct influence on the effective gravimetric hydrogen capacity. Thereby, only lightweight chemical elements and their compounds are promising for reaching DOE targets for onboard hydrogen storage.[4] Nevertheless, there are several materials that are potentially interesting for the reversible storage of hydrogen. In these, hydrogen can be stored in atomic and molecular form. In the former, during the absorption and desorption processes, chemical bonds need to be broken and formed, affecting the (de)hydrogenation kinetics.[5-7] For the latter, highly porous open structures decorated with lightweight metal atoms, with an effort to improve their interactions with hydrogen molecules[8-10], attracted significant interest in recent years.[11-14] Among these are the metal decorated, atomically thin two-dimensional (2D) materials. As for the candidate metal atom, Li is usually preferred due to its light atomic weight, and the relatively small cohesive energy, when compared to other candidate metals. Li decorated C[15-20], B[21-23], C&B[24-27], and C&N[28-31], 2D materials have been studied for hydrogen storage.

A completely new, atomically thin 2D material, B_2S, has very recently been predicted by Wang and co-workers using Particle Swarm Optimization method.[32] B_2S, with the same number of valence electrons as graphene, was predicted to have a honeycomb structure at its ground state. Li *et al.* have studied the Li and Na storage properties of 2D-B_2S monolayers and compared the key features of B_2S to the strained graphene.[33]

Performing *ab initio* Molecular Dynamics (AIMD) simulations, they found that the fully Li-covered B_2S monolayer was thermally stable at 400 K and was a good candidate anode material for both Li and Na batteries. In this paper, we present the results of our density functional theory (DFT) calculations for the study of hydrogen storage properties of single layer B_2S and Li-decorated single layer B_2S sheets with different Li loading concentrations.

2. Computational methods

DFT calculations were carried out using a plane-wave basis, as implemented in the Vienna *ab initio* simulation package (VASP)[34-36]. We used the projector augmented wave (PAW) method[37, 38] treating for H, Li, B, and S, one, three, three and six electrons, respectively, as valence. We employed the generalized gradient approximation (GGA), in the form of the Perdew−Burke−Ernzerhof (PBE)[39] functional. To account for the dispersion interactions, we used the DFT-D3 correction method of Grimme[40, 41] with its default force-field parameters. The PAW technique, PBE functional and the DFT-D3 correction scheme have been applied successfully for studying the interactions between different host materials and molecular hydrogen[41-44].

The kinetic energy cutoff for the plane-wave expansion of the electron wave functions was set at 500 eV. For all structural optimizations and the calculation of electronic properties of the optimized structures, we used Γ-centered 6 × 10 × 1 regular **k**-point grids[45]. A vacuum spacing of 20 Å was used to avoid interactions between monolayers. For the isolated H_2 molecule calculations, we used a 15 Å edge cubic box with periodicity. The relaxations of atomic positions were carried out with no spatial and symmetry constraints. The convergence criterion for self-consistency was set to

0.01 meV between two consecutive electronic steps. The structural optimizations of the structures were assumed to be complete when the total remaining forces on the atoms were lower than 0.01 eV/Å. The tetrahedron method with Blöchl corrections was applied for the calculation of electronic density of states (DOS).

We calculate the binding energy of Li atoms to the most stable atomic configuration B_2S monolayer, having the chemical formula of B_8S_4 in its primitive cell, as follows

$$E_b^{Li} = \left(xE_{Li} + E_{B_8S_4} - E_{B_8S_4Li_x}\right)/x \quad (1)$$

where E_{Li} is the total energy of an isolated Li atom, $E_{\mathrm{B_8S_4}}$ and $E_{\mathrm{B_8S_4Li}_x}$ are the total energies of the B_8S_4 primitive unit cells prior and posterior to Li decoration, respectively.

We calculate the consecutive and the average binding energies of H_2 molecules to the $B_8S_4Li_x$ compounds using **Equations (2)** and **(3)**, respectively.

$$E_b^{H_2-con} = E_{H_2} + E_{B_8S_4Li_xH_{2y-2}} - E_{B_8S_4Li_xH_{2y}} \quad (2)$$

$$E_b^{H_2-ave} = \left(yE_{H_2} + E_{B_8S_4Li_x} - E_{B_8S_4Li_xH_{2y}}\right)/y \quad (3)$$

where $E_{\mathrm{H_2}}$ and $E_{\mathrm{B_8S_4Li}_x\mathrm{H}_{2y}}$ are the total energies of the H_2 molecule and the stepwise hydrogenated $B_8S_4Li_x$ compounds, respectively.

3. Results and discussions

The optimized primitive cell of the B_2S monolayer is shown in **Figure 1(a)**. The orthogonal primitive cell contains four formula units and has cell parameters of a = 9.14, b = 5.26, and c = 20.00 Å, while the latter represents vacuum distance between monolayers. The optimized B–B and B–S bond lengths are 1.62 and 1.82 Å, respectively. These optimized lattice parameters and bond lengths are in accordance with the results of Wang *et al*.[32]

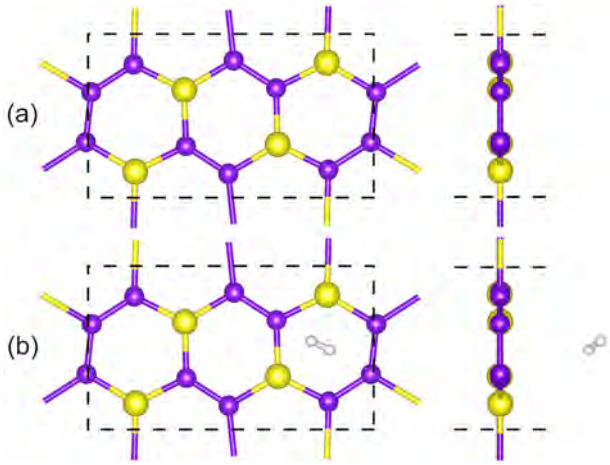

Figure 1. The top and side views of (a) the optimized B_2S primitive cell with four formula units and (b) the most stable geometry of H_2 molecule on B_2S monolayer. The purple, yellow and white spheres denote B, S and H atoms, respectively.

We first study the interaction of hydrogen molecule with the B_2S sheet by considering different absorption sites on B_2S, including the top of B and S atoms, top of B–B and B–S bond centers, and top of hexagonal ring centers, all with respect to the center of the molecule. We construct a total of twenty different H_2 configurations where the hydrogen molecules have been placed parallel to the B_2S sheet with its center of mass approximately 2 Å away from the surface. After structural optimizations, we find that the lowest energy configuration is when the H_2 molecule is residing over the center of hexagonal rings with an angle of approximately 30° from its axis to the monolayer, as shown in **Figure 1(b)**. The binding energy of the H_2 molecule is calculated as 0.08 eV/H_2, which is similar to the physisorption energy of H_2 on graphene[46, 47]. As shown in **Figure 1**, the structural integrity of the B_2S monolayer is not affected with the presence of H_2 molecules.

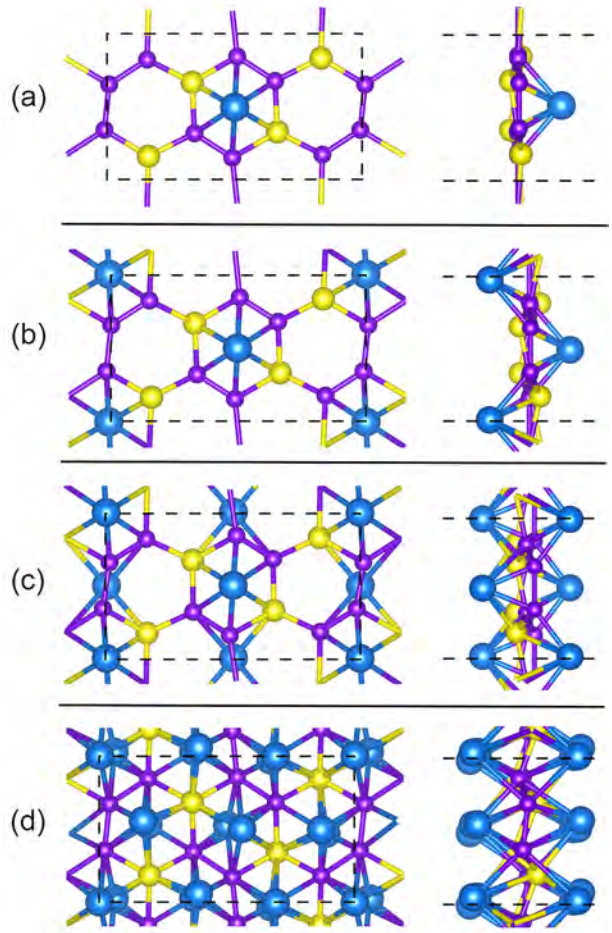

Figure 2. The most stable structures of (a) B_8S_4Li, (b) $B_8S_4Li_2$, (c) $B_8S_4Li_4$, and (d) $B_8S_4Li_{12}$ compounds. The Li atoms are shown as blue spheres.

Next, we study the interaction of Li atoms with the B_2S monolayer. For the functionalization of B_2S monolayer with a single Li atom, we consider different adsorption sites for Li, including over the hexagon centers, over the center of B–B and B–S bonds, and over the B and S atoms. The most stable position for Li is found to be over the *para*-hexagon center, with a calculated binding energy of 1.75 eV/Li. We also consider that both sides of the B_2S monolayer can be functionalized with additional Li atoms. The calculated average binding energies of Li atoms for the two-, four-, and twelve-atom decorated B_8S_4 cells are 1.89, 1.93, and 1.84 eV/Li, respectively. The optimized structures of $B_8S_4Li_x$ compounds are shown in **Figure 2**. The calculated

binding energies of Li atoms for all the $B_8S_4Li_x$ compounds are higher than 1.71 eV/Li, the DFT calculated cohesive energy of bulk Li. These results indicate that, within the studied loading concentrations, the $B_8S_4Li_x$ compounds are stable with respect to clustering of Li atoms on the monolayer surface. As seen in **Figure 2**, the B_2S monolayer can in principle be functionalized at all of its hollow sites with Li atoms. Although the incremental loading of Li atoms causes visible structural deformations on the B_2S monolayer, its structural integrity is not broken. The optimized $B_8S_4Li_{12}$ structure that is shown in **Figure 2(d)** is very similar to the formerly reported structure of the same compound by Li *et al*.[33] For the heavily Li-loaded $B_8S_4Li_{12}$ compound, the calculated distances between the first order neighbors of Li atoms range from 2.82 to 3.58 Å. Meanwhile, with the addition of twelve Li atoms to the B_8S_4 primitive cell, the average distance between neighboring hollow sites of the B_2S layer increases slightly from 3.04 to 3.06 Å. This is comparable to the Li–Li distance of 2.91 Å in bulk Li crystal, and it is almost 23% larger than the distance between the hollow sites of the hexagons in graphene[48], where the Li atoms are adsorbed with the lowest energy but they cannot easily form a densely packed Li monolayer.

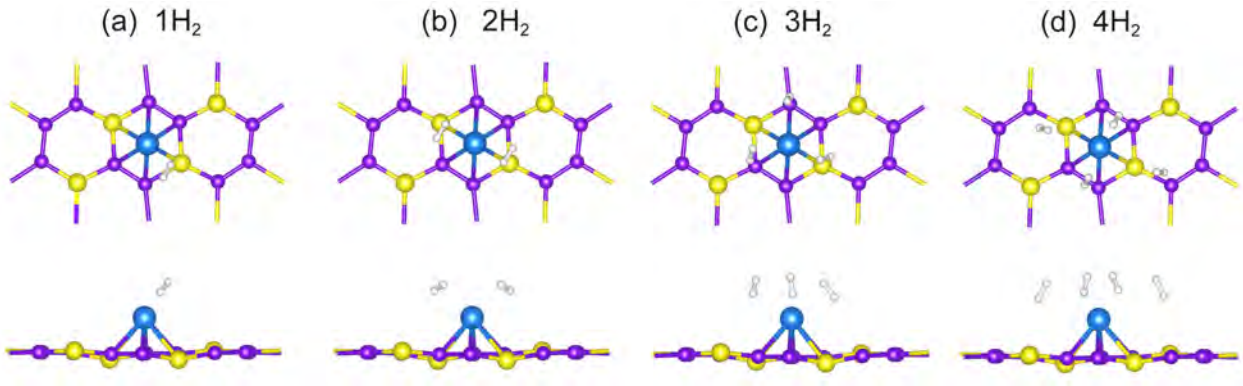

Figure 3. From (a) to (d), the side and top views of the optimized $B_8S_4LiH_{2y}$ (y = 1–4) compounds with gradually increasing amounts of hydrogen molecules.

Compound	$E_b^{H_2-con}$	$E_b^{H_2-ave}$	d_{Li-H_2}					d_{H-H}	Q_B	Q_S	Q_{Li}	Q_H
			1st H_2	2nd H_2	3rd H_2	4th H_2	ave					
B_8S_4Li									+0.53	-1.29	+0.87	
$B_8S_4LiH_2$	0.19	0.19	2.00				2.00	0.76	+0.54	-1.29	+0.87	-0.02
$B_8S_4LiH_4$	0.18	0.18	2.04	2.05			2.05	0.76	+0.55	-1.30	+0.86	-0.01
$B_8S_4LiH_6$	0.10	0.15	2.14	2.19	2.48		2.27	0.76	+0.55	-1.30	+0.88	-0.01
$B_8S_4LiH_8$	0.07	0.13	2.12	2.23	2.89	3.22	2.62	0.76	+0.55	-1.29	+0.88	-0.01

Table 1. The consecutive ($E_b^{H_2-con}$) and the average ($E_b^{H_2-ave}$) binding energies of H_2 molecules are given in eV/H_2. The Li–H_2 distances (d_{Li-H_2}) as measured from the center of the H_2 bonds and the H–H bond lengths (d_{H-H}) are given in Å. The average Bader charges per atom type of the $B_8S_4LiH_{2y}$ compounds are given in units of *e*.

After assessing the feasibility of Li decoration on B_2S, we then study the adsorption of H_2 molecules on Li decorated B_2S monolayers. For B_8S_4Li, the calculated consecutive and average binding energies of hydrogen molecules using the **Equations (2)** and **(3)**, respectively, are shown in **Table 1**. The first H_2 molecule binds with 0.19 eV to B_8S_4Li. The average binding energy of H_2 molecules decreases with each added hydrogen on the compound, finally dropping to 0.13 eV/H_2 for $B_8S_4LiH_8$. As shown in **Figure 3** and **Table 1**, up to three H_2 molecules can be accommodated around the protruding Li atom of the B_8S_4Li compound whose distances to metal, d_{Li-H_2}< 2.5 Å. Addition of the fourth hydrogen molecule is energetically feasible, though the consecutive binding energy, $E_b^{H_2-con}$, of the fourth H_2 molecule is only 0.07 eV/H_2. This value is similar to the calculated binding energy of the hydrogen molecule to the B_2S monolayer. Moreover, the optimized distance of the outermost H_2 molecule to Li atom is 3.22 Å. These results show that the interaction of the fourth H_2 molecule with the B_8S_4Li is

relatively weaker, and using this compound up to three H_2 molecules can effectively be stored, which results to $B_8S_4LiH_6$ with hydrogen content of 2.7 wt%. Therefore, both the thermodynamics and steric effects in relation to the exposed area of the metal atom determine the practical amount of H_2 molecules that can be stored[49].

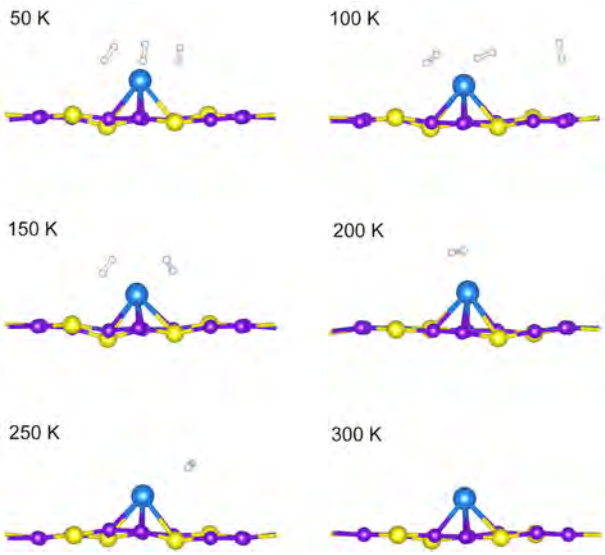

Figure 4. The snapshots from the side views of the $B_8S_4LiH_6$ compounds as obtained at the end of 20 ps AIMD simulations at T = 50, 100, 150, 200, 250, and 300 K.

Additionally, we carry out AIMD calculations[50] on the fully optimized $B_8S_4LiH_6$ compound to further study its stability and the dynamics during the hydrogen desorption process. AIMD calculations have been performed between the temperatures of 50 and 300 K, with 50 K intervals. During the AIMD simulations, the H_2 molecules that moved noticeably far away from the surface have been removed from simulation cells and the calculations have been carried on with the remaining H_2 molecules. **Figure 4** shows the structures at the end of 20 ps for six different AIMD runs. At 50 K, all the three H_2 molecules stay adsorbed on the Li atom. At 100 K, only one H_2 molecule has been found to depart away from the Li atom, but the molecule has stayed close to the surface,

with distances of < 3 Å to the surface, throughout the entire 20 ps. At T = 150 and 200 K, one and two H_2 molecules have been released from the $B_8S_4LiH_6$ compound, respectively. Similar to 200 K, at 250 K, only one H_2 molecule has remained adsorbed. However, unlike 200 K, at T = 250 K the $d_{\mathrm{Li-H_2}}$ distances has reached up to 2.8 Å during the simulation. Finally at T = 300 K, there are no H_2 molecules left on the B_8S_4Li compound. It is remarkable that for all the studied temperatures here, the B_8S_4Li compound was stable as in accordance with the previous results on the fully Li covered B_2S monolayers at 400 K[33]. In contrast to commonly studied atomic hydrogen storage materials, such as MgH_2[51-53], our AIMD calculations show that there are no kinetic barriers for hydrogen desorption from Li-decorated B_2S.

On both of the $B_8S_4Li_2$ and $B_8S_4Li_4$ compounds, up to three hydrogen molecules are adsorbed per Li, with average binding energies of 0.15 and 0.14 eV/H_2, respectively. For $B_8S_4Li_2$ and $B_8S_4Li_4$, this leads to noteworthy hydrogen storage capacities of 6.2 and 9.1 wt%, respectively. On the $B_8S_4Li_{12}$ compound, each Li atom of a densely packed Li monolayer interacts with a H_2 molecule via a significantly weaker average binding energy of 0.06 eV/H_2.

We further investigate the prior to lithiation and posterior to hydrogenation phases of the most interesting compound for hydrogen storage purposes, the $B_8S_4Li_4$, by calculating the electron localization functions (ELF)[37], performing Bader[54] charge analysis and the electronic density of states (DOS) calculations. Calculation of the ELF provides useful information about the electron distribution within the structure of the whole compound. In **Figure 5 (a–c)**, the optimized structures of the B_8S_4, $B_8S_4Li_4$, and $B_8S_4Li_4H_{24}$ compounds and their respective ELFs are shown. Clearly, all Li atoms are exposed on the B_2S monolayer and are depleted. Li atoms have no orbital interactions with the B_2S monolayer or the H_2 molecules around them. Additionally, the localized

electron clouds positioned around the H_2 molecules show no evidence of orbital interactions with the rest of the atoms of the host material. **Table 2** shows the decomposition of Bader charges onto the atoms of the B_8S_4, $B_8S_4Li_4$, and $B_8S_4Li_4H_{24}$ compounds. Similar to the ELF analysis, the Li atoms on the B_2S monolayer are depleted and they carry an effective positive charge of about 0.9 *e,* which is not affected by the (un)loading of hydrogen molecules. The Bader charge states of Li atoms on the B_2S monolayer have found to be similar to those of the Li atoms that decorated the boron sheets[21], showing the promise of the B_2S monolayer as a host material for immobilizing the Li atoms. The calculated charges on H atoms of the $B_8S_4Li_4H_{24}$ compound are close to zero, which shows that there is no remarkable charge transfer between the $B_8S_4Li_4$ and the H_2 molecules.

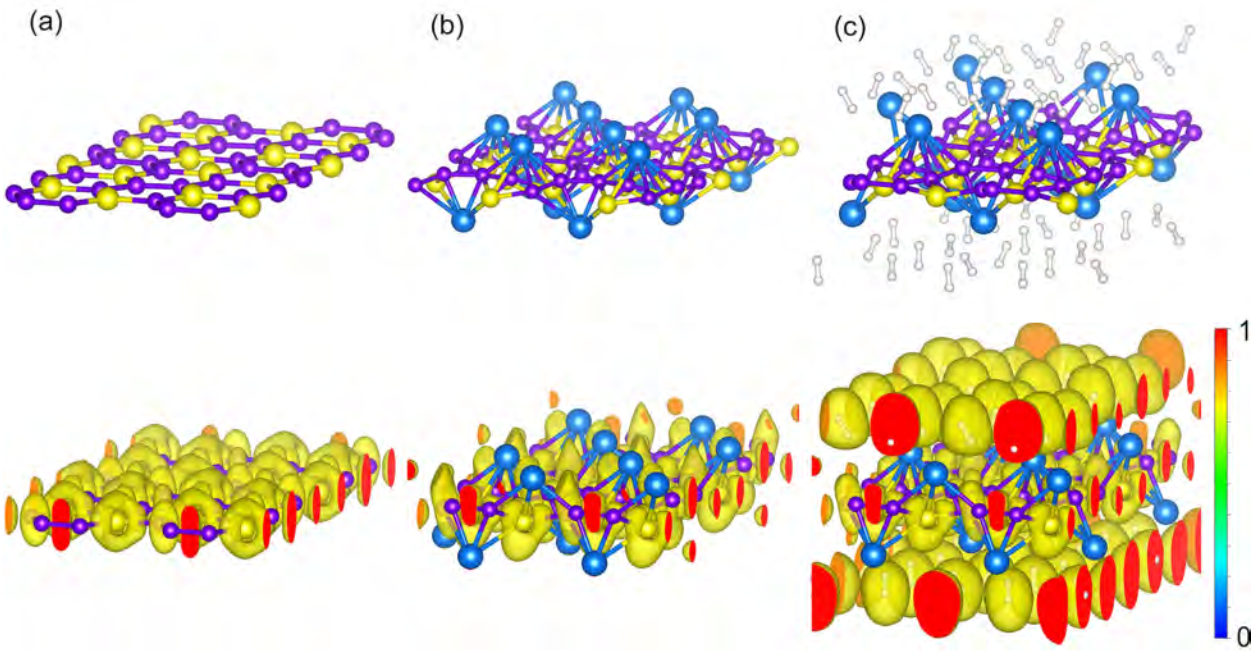

Figure 5. The perspective views of the optimized structures of (a) B_8S_4, (b) $B_8S_4Li_4$, (c) $B_8S_4Li_4H_{24}$ (top), and their corresponding ELF plots (bottom). Li, B, S, H atoms are shown as blue, purple, yellow and white spheres, respectively.

Compound	Q^{B}_{ave}	Q^{B}_{max}	Q^{B}_{min}	Q^{S}_{ave}	Q^{S}_{max}	Q^{S}_{min}	Q^{Li}_{ave}	Q^{Li}_{max}	Q^{Li}_{min}	Q^{H}_{ave}	Q^{H}_{max}	Q^{H}_{min}
B_8S_4	+0.63	+0.74	+0.48	-1.27	-1.27	-1.27						
$B_8S_4Li_4$	+0.24	+0.31	+0.17	-1.34	-1.34	-1.35	+0.86	+0.86	+0.86			
$B_8S_4Li_4H_{24}$	+0.28	+0.43	+0.13	-1.33	-1.33	-1.33	+0.88	+0.88	+0.88	-0.02	+0.04	-0.08

Table 2. Bader charge analysis of the DFT optimized B_8S_4, $B_8S_4Li_4$, and $B_8S_4Li_4H_{24}$ compounds. All charges are given in units of *e*.

Figure 6(a) shows the calculated electronic DOS of the B_8S_4 primitive cell (**Figure 5(a)**), which is in very good agreement with previous results[32]. When both sides of the monolayer are functionalized with the Li atoms, the $B_8S_4Li_4$ compound (**Figure 5(b))** is formed. Charge transfer, from the Li atoms to the monolayer, takes place as evidenced by both the ELF contours and the Bader charges. Confirming these two methods, **Figure 6(b)** shows the DOS for the $B_8S_4Li_4$ compound, in which the charge transfer from the Li atoms to the monolayer results in the population of the B_2S monolayer's originally empty conduction states of approximately between 0 and 2 eV. For $B_8S_4Li_4$, a similar result has also been observed by Li *et al*.[33] The calculated electronic DOS for the fully hydrogenated $B_8S_4Li_4$ (**Figure 5(c)**) is shown in **Figure 6(c).** As for $B_8S_4Li_4H_{24}$, the adsorbed H_2 molecules on the Li decorated B_2S monolayer populate the low energy states that are approximately between -7.5 and -10 eV. According to these findings, the presence of H_2 molecules does not influence the binding interactions between B, S, and Li atoms, consistent with our ELF and Bader charge analysis as discussed above. A closer inspection of the projected DOS shown in **Figure 6** reveals that there are no notable hybridizations between Li and the H orbitals and the loading of H_2 molecules onto the Li decorated B_2S has not affected the binding interactions between the constituting atoms of the storage material. These findings are

consistent with our ELF and Bader charge analysis as were discussed above, suggesting that the interactions between $B_8S_4Li_4$ and H_2 molecules are of electrostatic nature.

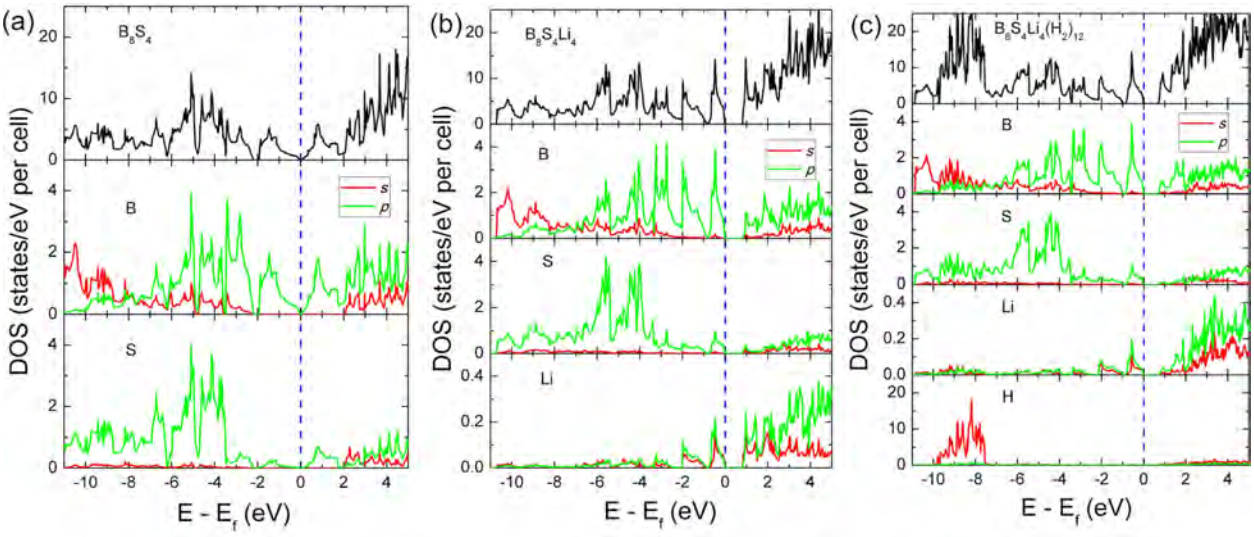

Figure 6. DFT calculated electronic DOS for the compounds (a) B_8S_4, (b) $B_8S_4Li_4$ and, (c) $B_8S_4Li_4H_{24}$. For each compound, total DOS are shown in black at the top of the figures, and the projected DOS onto the atoms with *s* and *p* contributions are shown in red and green, respectively. For all figures (a–c), the origin of energy is set at the highest occupied state and indicated with a vertical dashed blue line.

4. Conclusions

In summary, we performed DFT calculations to study the adsorption of H_2 molecules on B_2S and the Li decorated B_2S compounds. H_2 molecules were found to interact weakly, with a binding energy of 80 meV/H_2, with the atomically thin B_2S honeycomb monolayer. To increase the H_2 binding energies, we utilized the B_2S sheet as a substrate for immobilizing Li atoms. Unlike Li-decorated graphene, the 2D–B_2S interacts strongly with Li atoms and the Li decorated monolayers are thermodynamically stable, showing their promise for practical use. Among the studied $B_8S_4Li_x$ compounds, the

$B_8S_4Li_4$ yields the highest hydrogen storage capacity of 9.1 wt% H_2. For this compound, each protruding Li atom on the B_2S surface interacts up to three H_2 molecules via non-covalent interactions and with an average hydrogen binding energy of 0.14 eV/H_2. Our DFT calculations show that Li-decorated B_2S is a promising candidate material for molecular hydrogen storage.

Acknowledgements

We gratefully acknowledge funding by The Dutch Organisation for Internationalization in Education (NUFFIC) and the China Scholarship Council (CSC) for enabling ZL to perform his studies at DIFFER. SE acknowledges funding from the initiative "Computational Sciences for Energy Research" of Shell and the Netherlands Organisation for Scientific Research (NWO). Computational work was carried out on the Dutch national e-infrastructure with the support of SURF Cooperative.

Declaration of interest:

None

References

[1] Hydrogen on the rise. Nat Energy. 2016;1:1. https://doi.org/10.1038/nenergy.2016.127
[2] Schlapbach L, Züttel A. Hydrogen-storage materials for mobile applications. Nature. 2001;414:353. https://doi.org/10.1038/35104634
[3] Yang J, Sudik A, Wolverton C, Siegel DJ. High capacity hydrogen storage materials: attributes for automotive applications and techniques for materials discovery. Chem Soc Rev. 2010;39:656-75. https://doi.org/10.1039/B802882F
[4] DOE Technical Targets for Onboard Hydrogen Storage for LightDuty Vehicles. 2017.http://www.energy.gov/eere/fuelcells/doe-technical-targets-onboard-hydrogen-storage-light-duty-vehicles
[5] Er S, de Wijs GA, Brocks G. Tuning the Hydrogen Storage in Magnesium Alloys. Journal of Physical Chemistry Letters. 2010;1:1982-6. https://doi.org/10.1021/jz100386j
[6] Zhou C, Fang ZZ, Ren C, Li J, Lu J. Effect of Ti Intermetallic Catalysts on Hydrogen Storage Properties of Magnesium Hydride. Journal of Physical Chemistry C. 2013;117:12973-80. https://doi.org/10.1021/jp402770p

[7] Liu Z, Xiong L, Li J, Liu S, Er S. Effects of alloying elements (Al, Mn, Ru) on desorption plateau pressures of vanadium hydrides: An experimental and first-principles study. International Journal of Hydrogen Energy. 2018;43:21441-50. https://doi.org/10.1016/j.ijhydene.2018.09.204
[8] Kubas GJ. Fundamentals of H_2 Binding and Reactivity on Transition Metals Underlying Hydrogenase Function and H_2 Production and Storage. Chemical Reviews. 2007;107:4152-205. https://doi.org/10.1021/cr050197j
[9] Hoang TKA, Antonelli DM. Exploiting the Kubas Interaction in the Design of Hydrogen Storage Materials. Advanced Materials. 2009;21:1787-800. https://doi.org/10.1002/adma.200802832
[10] Skipper CVJ, Hoang TKA, Antonelli DM, Kaltsoyannis N. Transition Metal Hydrazide-Based Hydrogen-Storage Materials: the First Atoms-In-Molecules Analysis of the Kubas Interaction. Chemistry-a European Journal. 2012;18:1750-60. https://doi.org/10.1002/chem.201102715
[11] Lee H, Ihm J, Cohen ML, Louie SG. Calcium-Decorated Graphene-Based Nanostructures for Hydrogen Storage. Nano Letters. 2010;10:793-8. https://doi.org/10.1021/nl902822s
[12] Er S, de Wijs GA, Brocks G. Improved hydrogen storage in Ca-decorated boron heterofullerenes: a theoretical study. Journal of Materials Chemistry A. 2015;3:7710-4. https://doi.org/10.1039/C4TA06818A
[13] Tan X, Tahini HA, Smith SC. Computational design of two-dimensional nanomaterials for charge modulated CO_2/H_2 capture and/or storage. Energy Storage Materials. 2017;8:169-83. https://doi.org/10.1016/j.ensm.2016.12.002
[14] Kumar S, Samolia M, Dhilip Kumar TJ. Hydrogen Storage in Sc and Li Decorated Metal–Inorganic Framework. ACS Applied Energy Materials. 2018;1:1328-36. https://doi.org/10.1021/acsaem.8b00034
[15] Zhou W, Zhou J, Shen J, Ouyang C, Shi S. First-principles study of high-capacity hydrogen storage on graphene with Li atoms. Journal of Physics and Chemistry of Solids. 2012;73:245-51. https://doi.org/10.1016/j.jpcs.2011.10.035
[16] Guo Y, Jiang K, Xu B, Xia Y, Yin J, Liu Z. Remarkable Hydrogen Storage Capacity In Li-Decorated Graphyne: Theoretical Predication. Journal of Physical Chemistry C. 2012;116:13837-41. https://doi.org/10.1021/jp302062c
[17] Kim D, Lee S, Hwang Y, Yun K-H, Chung Y-C. Hydrogen storage in Li dispersed graphene with Stone–Wales defects: A first-principles study. International Journal of Hydrogen Energy. 2014;39:13189-94. https://doi.org/10.1016/j.ijhydene.2014.06.163
[18] Zhang X, Tang C, Jiang Q. Electric field induced enhancement of hydrogen storage capacity for Li atom decorated graphene with Stone-Wales defects. International Journal of Hydrogen Energy. 2016;41:10776-85. https://doi.org/10.1016/j.ijhydene.2016.05.053
[19] Wang F, Zhang T, Hou X, Zhang W, Tang S, Sun H, et al. Li-decorated porous graphene as a high-performance hydrogen storage material: A first-principles study. International Journal of Hydrogen Energy. 2017;42:10099-108. https://doi.org/10.1016/j.ijhydene.2017.01.121
[20] Alp IO, Aydin S, Ciftci YO. First-principles hydrogen adsorption properties of Li-decorated $ThMoB_4$-type graphene. International Journal of Hydrogen Energy. 2018;43:16117-27. https://doi.org/10.1016/j.ijhydene.2018.07.052
[21] Er S, de Wijs GA, Brocks G. DFT Study of Planar Boron Sheets: A New Template for Hydrogen Storage. Journal of Physical Chemistry C. 2009;113:18962-7. https://doi.org/10.1021/jp9077079
[22] Li J, Zhang H, Yang G. Ultrahigh-Capacity Molecular Hydrogen Storage of a Lithium-Decorated Boron Monolayer. Journal of Physical Chemistry C. 2015;119:19681-8. https://doi.org/10.1021/acs.jpcc.5b06164
[23] Ji Y, Dong H, Li Y. Theoretical Predictions on Li-Decorated Borophenes as Promising Hydrogen Storage Materials. Chemistryselect. 2017;2:10304-9. https://doi.org/10.1002/slct.201702203
[24] Park H-L, Yoo DS, Chung Y-C. Adsorption and Diffusion of Li and Ni on Graphene with Boron Substitution for Hydrogen Storage: Ab-initio Method. Japanese Journal of Applied Physics. 2011;50. https://doi.org/10.1143/jjap.50.06gj02
[25] An H, Liu C-s, Zeng Z, Fan C, Ju X. Li-doped B_2C graphene as potential hydrogen storage medium. Applied Physics Letters. 2011;98. https://doi.org/10.1063/1.3583465
[26] Park H-L, Yi S-C, Chung Y-C. Hydrogen adsorption on Li metal in boron-substituted graphene: An ab initio approach. International Journal of Hydrogen Energy. 2010;35:3583-7. https://doi.org/10.1016/j.ijhydene.2010.01.073
[27] Zhang Y, Cheng X. Hydrogen Storage on Li Coated BC_3 Honeycomb Sheet. Chinese Journal of Chemistry. 2017;35:1329-32. https://doi.org/10.1002/cjoc.201600911

[28] Wu MH, Wang Q, Sun Q, Jena PR. Functionalized Graphitic Carbon Nitride for Efficient Energy Storage. Journal of Physical Chemistry C. 2013;117:6055-9. https://doi.org/10.1021/jp311972f
[29] Lee S, Lee M, Choi H, Yoo DS, Chung Y-C. Effect of nitrogen induced defects in Li dispersed graphene on hydrogen storage. International Journal of Hydrogen Energy. 2013;38:4611-7. https://doi.org/10.1016/j.ijhydene.2013.01.180
[30] Hashmi A, Farooq MU, Khan I, Son J, Hong J. Ultra-high capacity hydrogen storage in a Li decorated two-dimensional C_2N layer. Journal of Materials Chemistry A. 2017;5:2821-8. https://doi.org/10.1039/c6ta08924k
[31] Chen Y-D, Yu S, Zhao W-H, Li S-F, Duan X-M. A potential material for hydrogen storage: a Li decorated graphitic-CN monolayer. Physical Chemistry Chemical Physics. 2018;20:13473-7. https://doi.org/10.1039/c8cp01145a
[32] Zhao Y, Li X, Liu J, Zhang C, Wang Q. A New Anisotropic Dirac Cone Material: A B_2S Honeycomb Monolayer. Journal of Physical Chemistry Letters. 2018;9:1815-20. https://doi.org/10.1021/acs.jpclett.8b00616
[33] Li P, Li Z, Yang J. Rational Design of Two-dimensional Anode Materials: B_2S as a Strained Graphene. Journal of Physical Chemistry Letters. 2018;9:4852-6. https://doi.org/10.1021/acs.jpclett.8b02035
[34] Kresse G, Hafner J. Ab initio molecular dynamics for open-shell transition metals. Physical Review B. 1993;48:13115-8. https://doi.org/10.1103/PhysRevB.48.13115
[35] Kresse G, Furthmuller J. Efficiency of ab-initio total energy calculations for metals and semiconductors using a plane-wave basis set. Computational Materials Science. 1996;6:15-50. https://doi.org/10.1016/0927-0256(96)00008-0
[36] Kresse G, Furthmuller J. Efficient iterative schemes for ab initio total-energy calculations using a plane-wave basis set. Physical Review B. 1996;54:11169-86. https://doi.org/10.1103/PhysRevB.54.11169
[37] Blochl PE. Projector augmented-wave method. Physical Review B. 1994;50:17953-79. https://doi.org/10.1103/PhysRevB.50.17953
[38] Kresse G, Joubert D. From ultrasoft pseudopotentials to the projector augmented-wave method. Physical Review B. 1999;59:1758-75. https://doi.org/10.1103/PhysRevB.59.1758
[39] Perdew JP, Burke K, Ernzerhof M. Generalized gradient approximation made simple. Physical Review Letters. 1996;77:3865-8. https://doi.org/10.1103/PhysRevLett.77.3865
[40] Grimme S, Antony J, Ehrlich S, Krieg H. A consistent and accurate ab initio parametrization of density functional dispersion correction (DFT-D) for the 94 elements H-Pu. Journal of Chemical Physics. 2010;132. https://doi.org/10.1063/1.3382344
[41] Grimme S. Density functional theory with London dispersion corrections. Wiley Interdisciplinary Reviews-Computational Molecular Science. 2011;1:211-28. https://doi.org/10.1002/wcms.30
[42] Lee K, Berland K, Yoon M, Andersson S, Schroder E, Hyldgaard P, et al. Benchmarking van der Waals density functionals with experimental data: potential-energy curves for H_2 molecules on Cu(111), (100) and (110) surfaces. Journal of Physics-Condensed Matter. 2012;24. https://doi.org/10.1088/0953-8984/24/42/424213
[43] Zeinalipour-Yazdi CD, Hargreaves JSJ, Laassiri S, Catlow CRA. DFT-D3 study of H_2 and N_2 chemisorption over cobalt promoted Ta_3N_5-(100), (010) and (001) surfaces. Physical Chemistry Chemical Physics. 2017;19:11968-74. https://doi.org/10.1039/c7cp00806f
[44] Bakhshi F, Farhadian N. Co-doped graphene sheets as a novel adsorbent for hydrogen storage: DFT and DFT-D3 correction dispersion study. International Journal of Hydrogen Energy. 2018;43:8355-64. https://doi.org/10.1016/j.ijhydene.2018.02.184
[45] Monkhorst HJ, Pack JD. Special points for Brillouin-zone integrations. Physical Review B. 1976;13:5188-92. https://doi.org/10.1103/PhysRevB.13.5188
[46] Heine T, Zhechkov L, Seifert G. Hydrogen storage by physisorption on nanostructured graphite platelets. Physical Chemistry Chemical Physics. 2004;6:980-4. https://doi.org/10.1039/b316209e
[47] Arellano JS, Molina LM, Rubio A, Alonso JA. Density functional study of adsorption of molecular hydrogen on graphene layers. Journal of Chemical Physics. 2000;112:8114-9. https://doi.org/10.1063/1.481411
[48] Liu Y, Artyukhov VI, Liu M, Harutyunyan AR, Yakobson BI. Feasibility of Lithium Storage on Graphene and Its Derivatives. Journal of Physical Chemistry Letters. 2013;4:1737-42. https://doi.org/10.1021/jz400491b
[49] Long J, Li J, Nan F, Yin S, Li J, Cen W. Tailoring the thermostability and hydrogen storage capacity of Li decorated carbon materials by heteroatom doping. Appl Surf Sci. 2018;435:1065-71. https://doi.org/10.1016/j.apsusc.2017.10.196

[50] Marc D, Hutter J. Ab Initio Molecular Dynamics: Theory and Implementation. John von Neumann Institute for Computing, Julich2000.
[51] Mushnikov NV, Ermakov AE, Uimin MA, Gaviko VS, Terent'ev PB, Skripov AV, et al. Kinetics of interaction of Mg-based mechanically activated alloys with hydrogen. Phys Metals Metallogr. 2006;102:421-31. https://doi.org/10.1134/s0031918x06100097
[52] Rahman MW. A review on on–board challenges of magnesium–based hydrogen storage materials for automobile applications. AIP Conference Proceedings. 2017;1851:020093. https://doi.org/10.1063/1.4984722
[53] Yahya MS, Ismail M. Synergistic catalytic effect of $SrTiO_3$ and Ni on the hydrogen storage properties of MgH_2. International Journal of Hydrogen Energy. 2018;43:6244-55. https://doi.org/10.1016/j.ijhydene.2018.02.028
[54] Henkelman G, Arnaldsson A, Jonsson H. A fast and robust algorithm for Bader decomposition of charge density. Computational Materials Science. 2006;36:354-60. https://doi.org/10.1016/j.commatsci.2005.04.010